Ductal pancreatic cancer modeling and drug screening using human pluripotent stem cell and patient-derived tumor organoids

Ling Huang[1], Audrey Holtzinger[1,2,11], Ishaan Jagan[1,11], Michael BeGora[1], Ines Lohse[1], Nicholas Ngai[1], Cristina Nostro[1,2], Rennian Wang[3], Lakshmi B. Muthuswamy[1], Howard C. Crawford[4], David W. Hedley[1], Cheryl Arrowsmith[1], Steve E. Kalloger[5,6,7] Daniel J. Renouf[6,7,8], Ashton A Connor[9], Sean Cleary[9], David F. Schaeffer[5,6,7], Michael Roehrl[1,] Ming-Sound Tsao[1,10], Steven Gallinger[9], Gordon Keller[1,2] and Senthil K. Muthuswamy[1,12]

[1]Princess Margaret Cancer Center, University Health Network (UHN), University of Toronto, Toronto, ON, Canada

[2]McEwen Center for Regenerative Medicine, University Health Network, Toronto, ON, Canada

[3]Departments of Physiology & Pharmacology, Western University, London, ON, Canada

[4]Mayo Clinic Cancer Center, Mayo Clinic, Jacksonville, FL, USA

[5]Division of Anatomic Pathology, Vancouver General Hospital, Vancouver, BC, Canada

[6]The University of British Columbia, Vancouver, BC, Canada

[7]Pancreas Centre BC, Vancouver, BC, Canada

[8]Division of Medical Oncology, BC Cancer Agency, Vancouver, BC, Canada

[9]Dvision of General Surgery, University of Toronto, Toronto, ON, Canada

[10]Department of Pathology, University Health Network, Toronto, ON, Canada

[11]These authors contributed equally

[12]Corresponding author: s.muthuswamy@utoronto.ca

Supplemental Figures

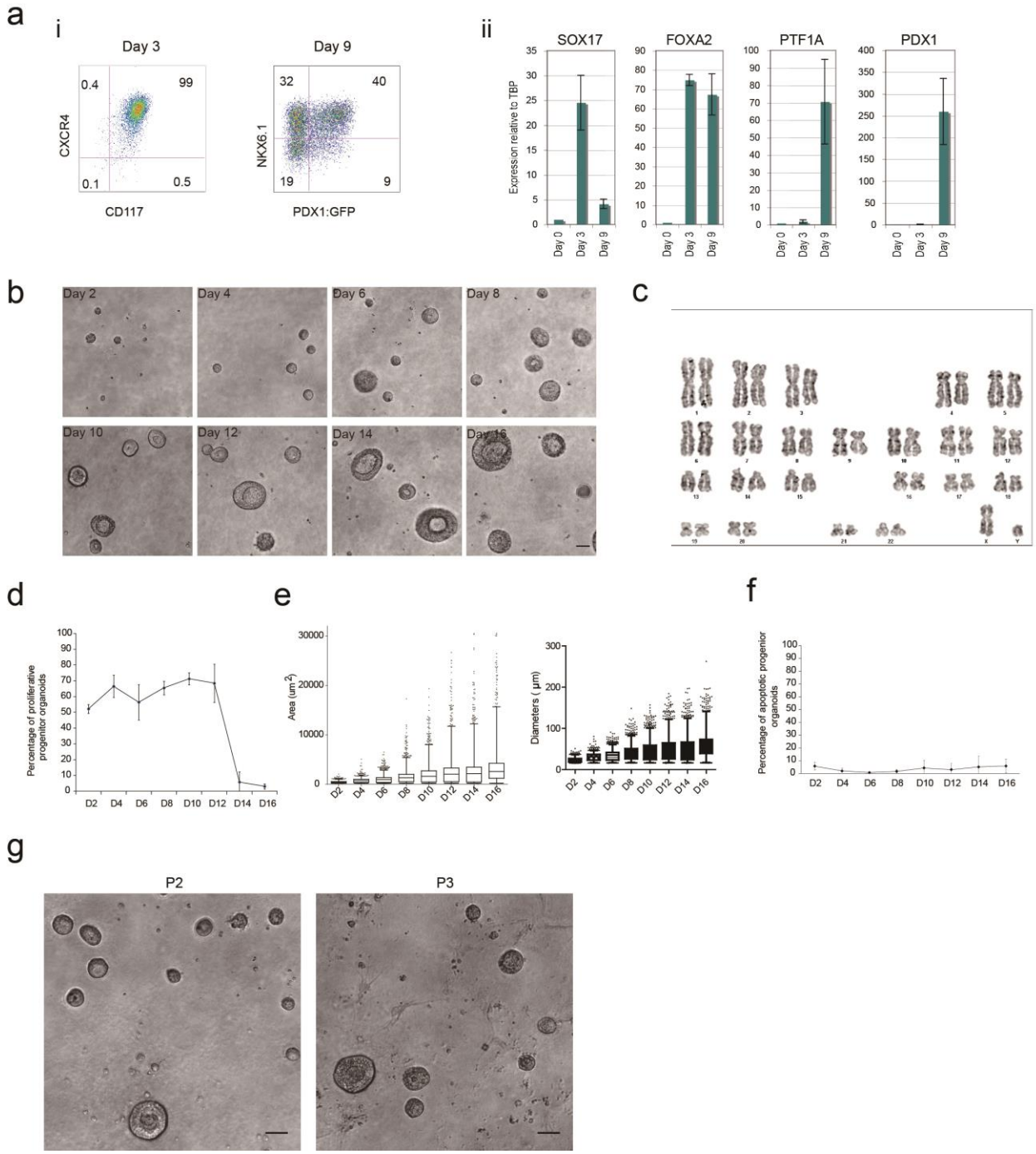

Supplemental Figure 1 Differentiation and morphogenesis of polarized organoids from induced progenitors. (**a**) Induction of pancreatic lineage cells. i) Flow cytometric validation of efficient definitive endoderm induction from MEL1-derived PDX1-GFP hESC by co-expression of CXCR4 and CD117 (T_3, left panel). Flow cytometric analysis of PDX1-GFP and NKX6.1 expression in day 9 multipotent pancreatic progenitors (T_9, right panel). ii) Real time PCR analysis for SOX17, FOXA2, PTF1A and PDX1 expression in hESCs (T_0), definitive endoderm

(T_3), and multipotent pancreatic progenitors (T_9, day 0 for 3D culture), (n=3, data represent mean +/- S.E.M). (**b**) Time sequence of organoid morphogenesis. Images were taken every 2 days with a phase contrast microscope. Scale bar, 50 μm. (**c**) Karyotype of cells in Day 16 Pancreatic Progenitor Organoids. All metaphase cells karyotyped (5/5) showed 46 chromosomes with normal diploid male human karyotype. (**d**) Quantification of Ki67 positive organoids during 3D morphogenesis. An organoid was counted as proliferative when more than 5% of cells in the organoid were positive for Ki67 staining. Graph summarizes results from three independent sets of experiments with over 100 structures counted in each experiment. (**e**) Changes in organoid size during morphogenesis as depicted in areas (left chart) or diameters (right chart). Data are presented as box plots. The box represents the interquartile range between first and third quartile and the median value represented by a solid line. The whiskers, 5% and 95% percentiles of the measurements; box top, third quartiles of measurements; box bottom, first quartile of the measurements; center line, median measurements. (**f**) Quantification of apoptotic organoids at different days in 3D culture. An organoid was counted as apoptotic when at least one apoptotic cell was present. Graph summarizes results from three independent sets of experiments with over 100 structures counted in each experiment. (**g**) Morphology of organoids from passage 2 and passage 3 as observed by a phase contrast microscope. Scale bar, 50 μm.

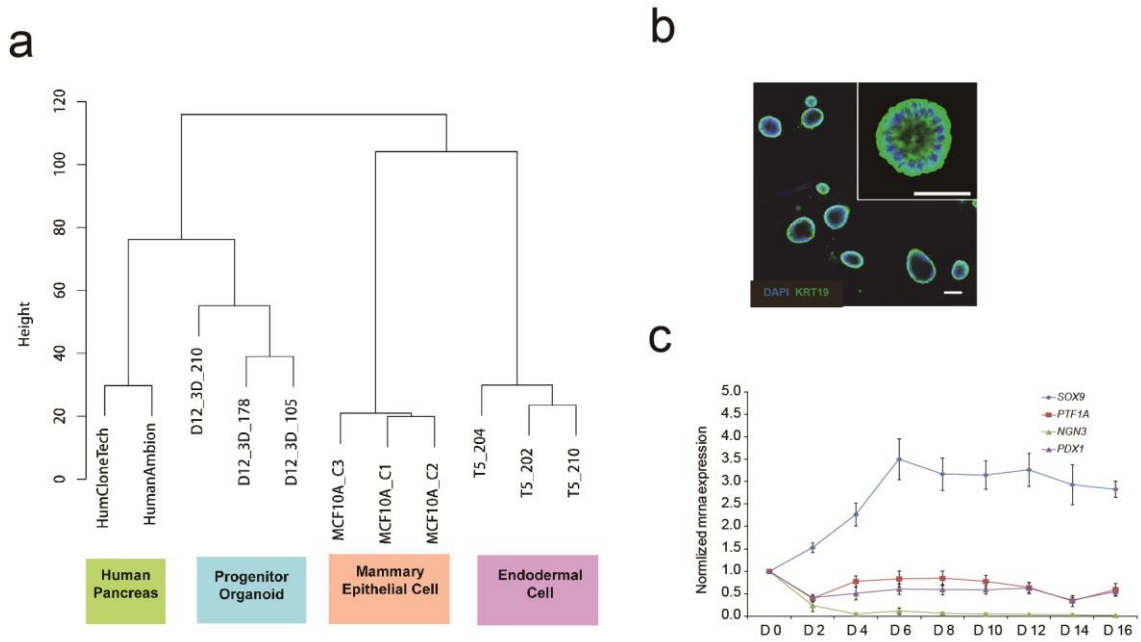

Supplemental Figure 2 Formation 3d organoids by pancreatic exocrine epithelial cells (**a**) Global gene expression in progenitor organoids. Gene expressions in pancreatic progenitor organoids, human adult pancreas, mammary epithelial cells line MCF-10A and definitive endoderm cells were detected by Illumina HT12 V4 Expression BeadChip. Dendrogram showed unsupervised clustering of pancreatic progenitor organoids close to human adult pancreas. (**b**) Expression of cytokeratin 19 (KRT19) in pancreatic progenitor organoid. All progenitor-organoids expressed pancreatic ductal epithelial cytokeratin KRT19. Insert, high resolution image of one organoid. DAPI, blue; KRT19, green. Scale bar, 50 µm. (**c**) Expression of markers associated with progenitor cells during 3D morphogenesis. The chart summarizes experiments from three independent experiments (data represent mean +/- S.E.M).

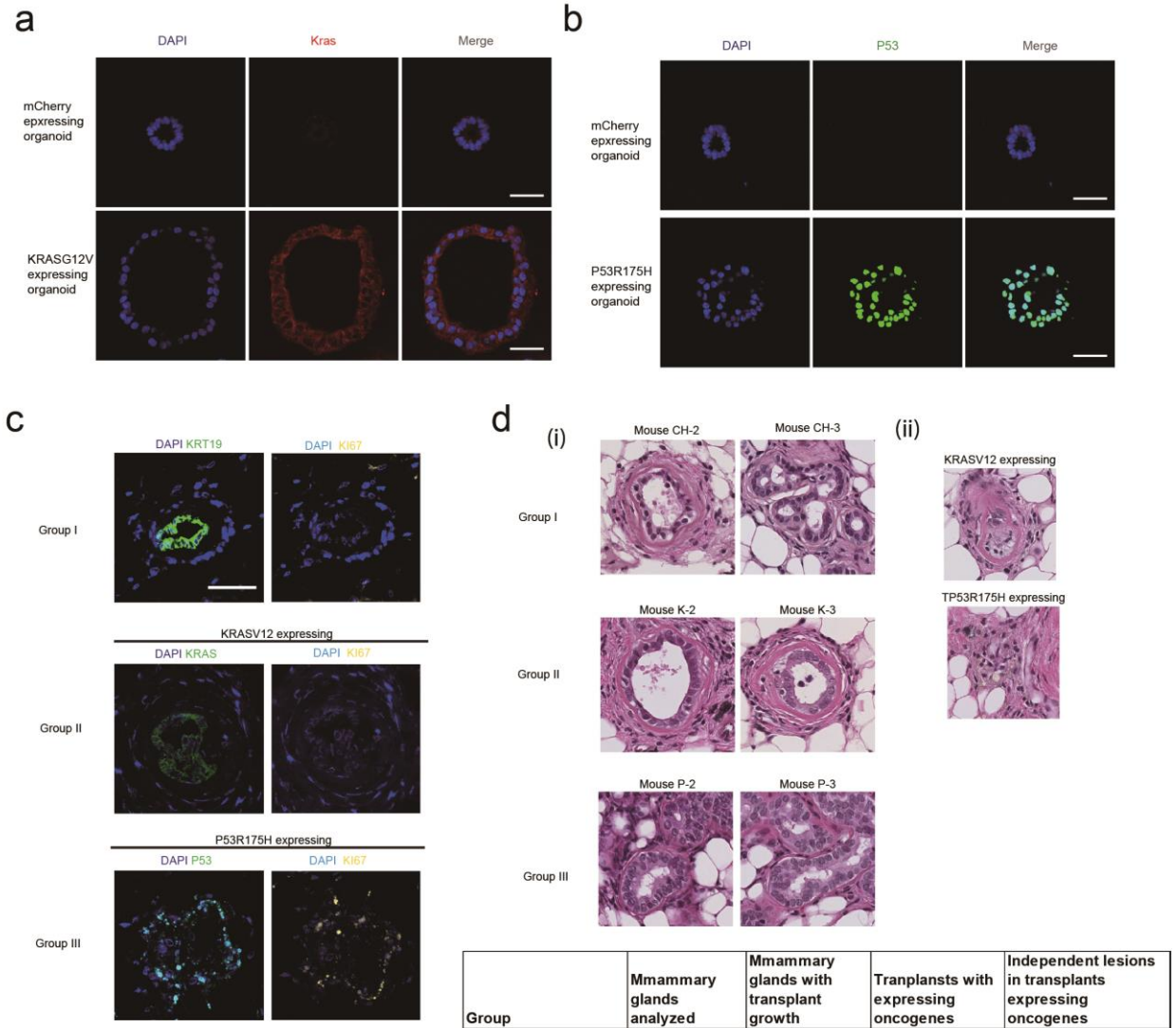

Group	Mmammary glands analyzed	Mmammary glands with transplant growth	Tranplansts with expressing oncogenes	Independent lesions in transplants expressing oncogenes
Group I (mCherry)	10	3	NA	NA
Group II (KRASG12V)	8	3	1	2
Group III (TP53R175H)	10	3	1	2

Supplemental Figure 3 Expression of KRAS and TP53 in progenitor-organoids. (**a**) Expression of KRAS in progenitor-organoids. KRAS, red; DAPI, blue. (**b**) Expression of P53 in progenitor-organoids. P53, green; DAPI, blue. Scale bars, 50 μm. (**c**) Human transplants outgrowths in mouse mammary glands, from progenitor-organoids expressing transgenes. Group I, progenitors transduced with mCherry: DAPI, blue; Keratin 19, green; KI67, yellow. Group II, progenitors transduced with KRASG12V: DAPI, blue; KRAS, green; KI67, yellow. Group III, progenitors transduced with TP53R175H: DAPI, blue; P53, green; KI67, yellow. (**d**) Outgrowth derived from transplantation of progenitor-organoids expressing transgenes. Image (i) shows H&E images of outgrowths in addition to those in **Fig. 4f**. Outgrowths in K-2, K-3, P-2 and P-3 mice did not express the transgene and had normal morphology. Image (ii) shows lesions identified in transgene expressing transplants, in addition to those shown in **Fig. 4f**. Table summarizes the transplantation experiment. Among the 8-10 mammary glands transplanted with cells from each group, three established outgrowths. Of the three, one transplant expressed

transgene whereas two were negative. The transgene-expressing transplant had two lesions for KRAS and two lesions for TP53. All four lesions showed abnormal histopathology, whereas all transgene-negative, but HLA-positive, outgrowths showed normal ductal morphology. All mCherry positive structures had normal duct morphology.

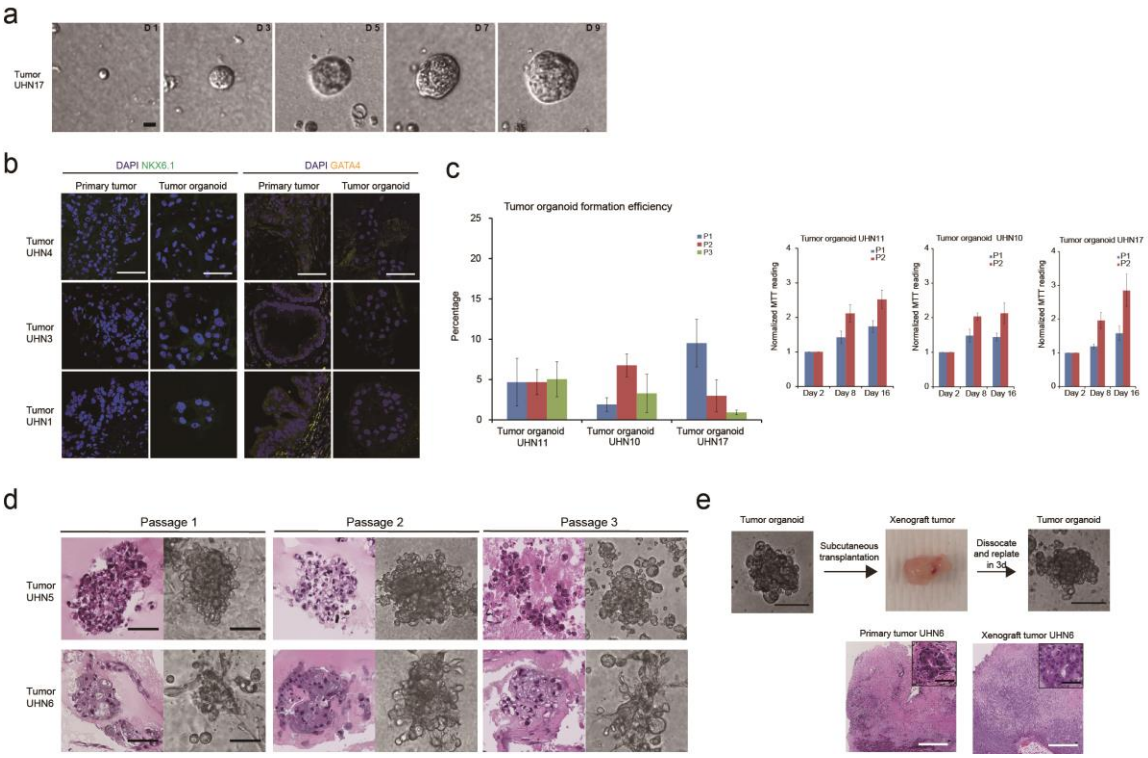

Supplemental Figure 4 Tumor organoid culture from fresh resections (**a**) Imaging sequence of UHN17 organogenesis. (**b**) Expression of NKX6.1 and GATA4 were undetectable in cell nuclei of primary tumors and corresponding tumor-organoids. DAPI, blue; NKX6.1, green; GATA4, yellow. (**c**) Percent tumor-organoid forming efficiency across three different passages (left panel) and MTT readings across multiple days for tumor-organoids used in top panel (right panels). (**d**) H&E and phase images of tumor-organoids frozen and thawed across multiple passages. (**e**) Propagation of tumor organoids *in vivo* and *in vitro*. Day 16 tumor organoids were dissociated and injected subcutaneously into flanks of NSG mice. Xenograft tumors were observed after 4-7 weeks. Xenograft tumors were then isolated and dissociated to re-seed in 3D. Tumor organoids grew from xenografts showed morphology consistent to original tumor organoids. The lower panel shows the histology of primary tumors from resection (left) and xenograft tumors (right). All scale bars equal to 50 μm.

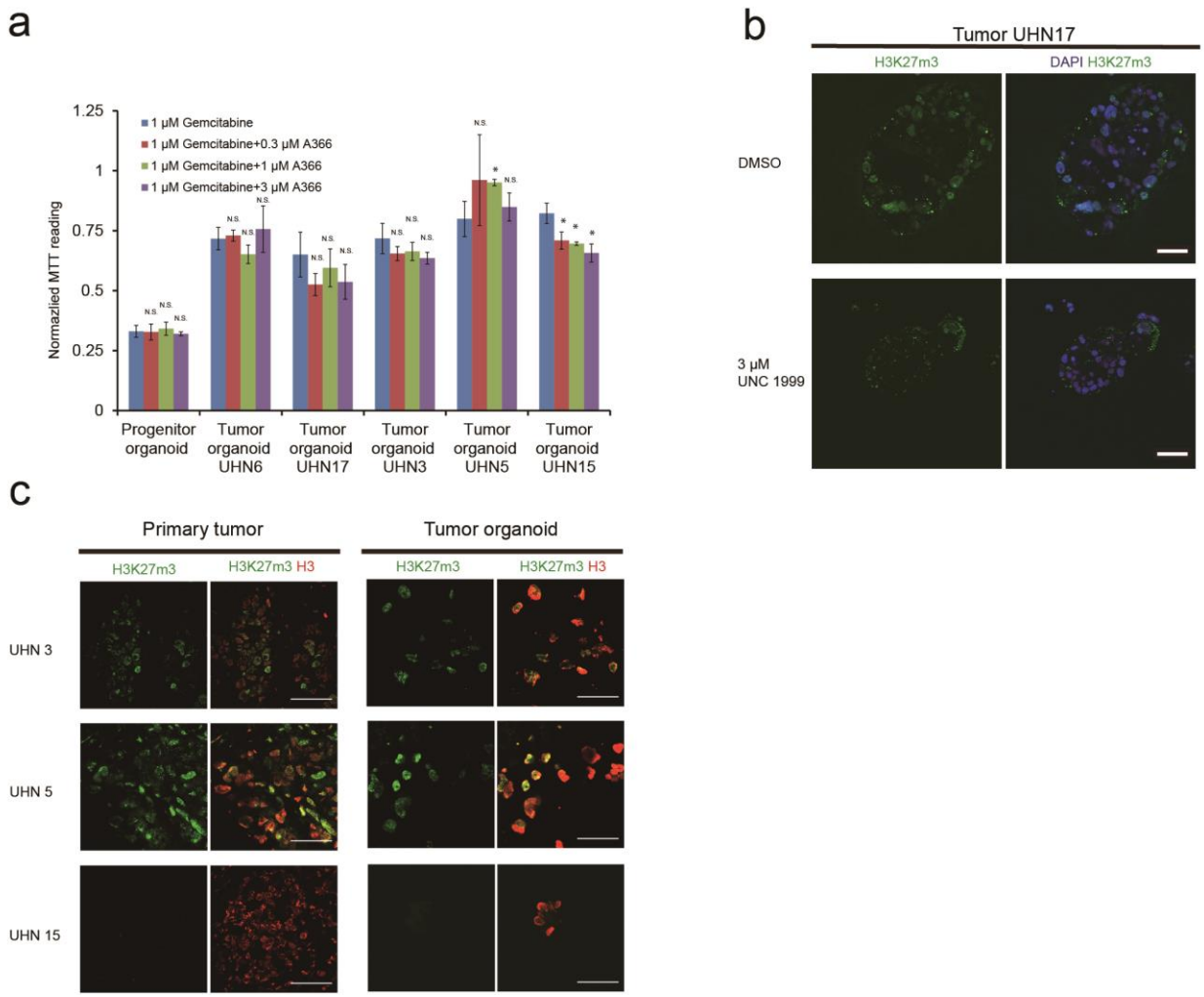

Supplemental Figure 5 Tumor organoids responses to therapeutic treatments (**a**) Normalized MTT assay readings of organoid cultures with gemcitabine and epigenetic inhibitors of the H3K9me2 writer *G9a* (A366). For MTT and oxygen consumptions experiments, data represent mean +/- S.D. P value (t-test, two tailed): N.S-, not significant; * P = 0.01 - 0.05; ** P = 0.001 - 0.01; *** P= < 0.001 (n=3). (**b**) Immunostaining for H3K27me3 in control (DMSO) or UNC 1999-treated tumor-organoids. DAPI, blue. Scale bars, 50μm. (**c**) Primary tumors (top panel) and tumor-organoids (bottom panel) derived from tumor UHN3, UHN 5 and UHN15, show consistent patient-specific variation in staining for Histone 3 (red) and H3K27me3 (green). Scale bars, 50μm.

Analysis of SOX9 Localization against clinicopathologic parameters.

Clinicopathologic Variable		Nuclear	Cytoplasmic	Negative	N v C Comparison
Age - Mean [Median]		65.9 [66.4]	67.7 [65.7]	63.4 [60.3]	$p_{Kruskal\text{-}Wallis} = 0.5945$
Sex	Male	113 (52.6%)	18 (75.0%)	1 (33.3%)	$p_{Fisher's\ Exact} = 0.0502$
	Female	102 (47.4%)	6 (25.0%)	2 (66.7%)	
Pathologic T-Stage	pT1	2 (0.9%)	0 (0%)	0 (0%)	$p_{Fisher's\ Exact} = 0.6145$
	pT2	12 (5.6%)	0 (0%)	0 (0%)	
	pT3	198 (93.0%)	23 (100%)	3 (100%)	
	pT4	1 (0.5%)	0 (0%)	0 (0%)	
Lymphovascular Invasion	Pos	115 (53.7%)	17 (73.9%)	2 (66.7%)	$p_{Fisher's\ Exact} = 0.0781$
	Neg	99 (46.3%)	6 (26.1%)	1 (33.3%)	
Perineural Invasion	Pos	195 (91.6%)	21 (91.3%)	3 (100%)	$p_{Fisher's\ Exact} = 1.0000$
	Neg	18 (8.4%)	2 (8.7%)	0 (0%)	
Regional Lymph Node Status	pN0	56 (26.3%)	3 (13.0%)	1 (33.3%)	$p_{Fisher's\ Exact} = 0.2083$†
	pN1	154 (72.3%)	20 (87.0%)	2 (66.7%)	
	pNX	3 (1.4%)	0 (0%)	0 (0%)	
Adjuvant Chemotherapy	Yes	68 (32.2%)	4 (16.7%)	0 (0%)	$p_{Fisher's\ Exact} = 0.1607$
	No	143 (67.8%)	20 (83.3%)	3 (100%)	
Tumor Grade	1	3 (1.4%)	0 (0%)	0 (0%)	$p_{Fisher's\ Exact} = 0.0433$ ‡
	2	162 (75.7%)	13 (56.5%)	2 (66.7%)	
	3	49 (22.9%)	10 (43.5%)	1 (33.3%)	

Each analyses used all availabe data so the total number of cases evaluated may differ across clinicopathologic variables.
† - The 3 cases with pNX recorded for regional lymph node status were excluded in this analysis.
‡ - The 3 cases with Grade 1 disease were excluded in this analysis.

Multivariable Disease Specific Survival For SOX9 Localization in PDAC

Clinicopathologic Covariates	Levels	Risk Ratio	95% CI	p-value
Age at Surgery	Entire range of regressor	1.86	0.80 - 4.34	0.1494
Sex	Male v Female	1.09	0.79 - 1.51	0.5935
Adjuvant Chemotherapy	Treated v Untreated	0.50	0.34 - 0.72	0.0002
Lymphovascular Invasion	Present v Absent	1.28	0.91 - 1.83	0.1597
Perineural Invasion	Present v Absent	1.89	0.97 - 4.17	0.0629
pT-Stage	pT4 v pT3	0.37	0.02 - 1.80	0.7028
	pT4 v pT2	0.34	0.02 - 2.01	
	pT4 v pT1	0.30	0.01 - 3.28	
	pT3 v pT2	0.91	0.45 - 2.10	
	pT3 v pT1	0.79	0.24 - 4.91	
	pT2 v pT1	0.87	0.21 - 5.87	
Regional Lymph Nodes pN-Stage	pN1 v pN0	2.23	1.47 - 3.45	< 0.0001
Tumor Grade	3 v 2	1.55	1.07 - 2.22	0.0417
	3 v 1	3.54	0.73 - 63.89	
	2 v 1	2.28	0.48 - 40.91	
SOX9 Localization	Cytoplasmic v Nuclear	1.07	0.62 - 1.75	0.8120

SOX9 Localization is not an independently prognostic marker due in part to its association with Tumor Grade and Lymphovascular Invasion.

Supplemental Table 1 Clinical significance of sox9 subcellular localizations The two tables show analysis of SOX9 localizations against clincopathologic parameters and the significance of multivariable disease specific survival for SOX localization in PDACs in cohort II. Patients who underwent curative surgical resection of histologically confirmed pancreatic adenocarcinoma who provided consent to tissue and molecular research were included in the studies. Patients were excluded if they had been lost to follow-up or died within 90 days of their surgical resection.

Supplemental Table 2 Information of patients

The table describes clinical information of patients whose tumor tissues were used in tumor organoid generation.

Patient IDs	Biobank ICGC Consent	Gender	Age	Incidental Finding	Incidental Finding Details	Other Findings	Pathology Tumor Site	Histological Type	Histological Grade	Tumor Size1	Tumor Size2	Tumor Size3	Invasion Type 1	Invasion Type 2	Invasion Type 3	Invasion Type 4	Invasion Type 5	Margins	RevisedMarginsSubmitted
UHN1	Y	F	59	FALSE			Pancreatic Head (C25.0)	Ductal adenocarcinoma	Moderately differentiated	3.8	2.4	2.1	Lymphatic/vascular Invasion	Perineural Invasion	extra pancreatic extension			Involved	NO
UHN2	Y	F	75	FALSE			Pancreatic Head (C25.0)	Ductal adenocarcinoma	Moderately differentiated	3.7	3.3	2.8	No Invasion Found					Uninvolved	NO
UHN3	Y	F	79	FALSE			Pancreatic Head (C25.0)	Ductal adenocarcinoma	Moderately differentiated	2.4	2	1.3	common bile duct Invasion	Lymphatic/vascular Invasion	Perineural Invasion			Uninvolved	NO
UHN4	Y	F	60	FALSE			Pancreatic Head (C25.0)	Ductal adenocarcinoma	Moderately differentiated	2.5	2.4	2	common bile duct Invasion	duodenal Invasion	extra pancreatic extension	Lymphatic/vascular Invasion	Perineural Invasion	Uninvolved	NO
UHN5	Y	F	66	FALSE			Pancreatic Head (C25.0)	Ductal adenocarcinoma	Poorly differentiated	3.2	2.6	2.3	Lymphatic/vascular Invasion	Perineural Invasion	extra pancreatic extension			Uninvolved	NO
UHN6	Y	F	52	TRUE	F/U on thyroid cancer	Satiety/Pain after eating	Pancreatic Head (C25.0)	Ductal adenocarcinoma	Poorly differentiated	5	4.5	4	Lymphatic/vascular Invasion	Perineural Invasion	Stomach Invasion	superior mesenteric vein Invasion	extra pancreatic extension	Uninvolved	NO
UHN7	Y	F	77	TRUE	CT Screening		Pancreatic Head (C25.0)	Ductal adenocarcinoma	Moderately differentiated	4	3	2.4	duodenal Invasion	extra pancreatic extension	Lymphatic/vascular Invasion	Perineural Invasion		Involved	NO
UHN8	Y	M	78	TRUE	F/U on chronic pancreatitis and IPMN		Pancreatic Head/Body/Tail	IPMN-Intestinal Type, Main Duct Type	Not specified/Unknown	5.8	7		duodenal Extension					Uninvolved	NO
UHN9	Y	F	67	FALSE			Pancreatic Head (C25.0)	Ductal adenocarcinoma	Moderately differentiated	2.8	2.3	1.8	Perineural Invasion	Lymphatic/vascular Invasion	common bile duct Invasion	extra pancreatic extension		Uninvolved	NO
UHN10	Y	F	68	TRUE	Abnormal Liver Functions		Pancreatic Head (C25.0)	Ductal adenocarcinoma	Well differentiated	3.8	3.7	3.2	Perineural Invasion	Lymphatic/vascular Invasion	extra pancreatic extension	duodenal Invasion		Involved	NO
UHN11	Y	M	65	FALSE		Anorexia/Lethargic	Pancreatic Head & Uncinate Process	Invasive Mucinous Cystic Neoplasm	Moderately differentiated	4	4	3	superior mesenteric vein Invasion	duodenal Invasion	extra pancreatic extension	Lymphatic/vascular Invasion Indeterminate	Perineural Invasion	Involved	NO
UHN12	Y	M	67	FALSE		Loose Bowel Movements	Pancreatic Head (C25.0)	Ductal adenocarcinoma	Moderately differentiated	4.8	4.7	4.2	Perineural Invasion	Lymphatic/vascular Invasion	duodenal Invasion			Uninvolved	NO
UHN13	Y	F	62	FALSE		Diarrhea	Pancreatic Head & Uncinate Process	Ductal adenocarcinoma	Moderately differentiated	1.4	1	0.9	extra pancreatic extension	Lymphatic/vascular Invasion	Perineural Invasion	common bile duct Invasion		Uninvolved	NO
UHN14	Y	F	51	FALSE			Pancreatic Head (C25.0)	Ductal adenocarcinoma	Not specified/Unknown	3.5	2.8	2	duodenal Invasion	Perineural Invasion	common bile duct Invasion	Lymphatic/vascular Invasion	extra pancreatic extension	Uninvolved	NO
UHN15	Y	M	59	FALSE			Pancreatic Head/Uncinate Process/Duodenal Wall/MV	Ductal adenocarcinoma	Moderately differentiated	4	3.7	1.9	Ampulla of Vater or Sphincter of Oddi Invasion	extra pancreatic extension	Lymphatic/vascular Invasion	Perineural Invasion	superior mesenteric vein Invasion	Uninvolved	NO
UHN16	Y	M	76	FALSE			Pancreatic Head (C25.0)	Ductal adenocarcinoma	Moderately differentiated	3	3	1.7	extra pancreatic extension	Lymphatic/vascular Invasion	Ampulla of Vater or Sphincter of Oddi Invasion	Perineural Invasion		Uninvolved	NO
UHN17	Y	F	46	FALSE			Pancreatic Head & Uncinate Process	Ductal adenocarcinoma	Moderately differentiated	2.8	2.3	2.2	extra pancreatic extension	Lymphatic/vascular Invasion	Perineural Invasion			Involved	NO
UHN18	Y	M	69	TRUE	Annual Physical		Pancreatic Neck (C25.7)	Ductal adenocarcinoma	Moderately differentiated	2.1	1.9	1.5	Lymphatic/vascular Invasion	Perineural Invasion				Uninvolved	NO
UHN19	Y	M	58	FALSE			Pancreatic Head (C25.0)	Ductal adenocarcinoma	Moderately differentiated	4.4	3	3.8	Perineural Invasion	duodenal Invasion	extra pancreatic extension			Uninvolved	NO
UHN20	Y	M	63	FALSE		Change in stool (NOS)	Pancreatic Head (C25.0)	Favor Acinar Cell	Poorly differentiated	3	2.7	2.5	Perineural Invasion	Lymphatic/vascular Invasion	extra pancreatic extension			Uninvolved	NO

Epigenetic Modifiers	**Targets**
JQ1	BET
LAQ824	histone deacetylase
SGC0946	DOT1L
A366	G9a
UNC1999	EZH2

Supplemental Table 3 Epigenetic modifiers tested in progenitor-organoids and their targets

Supplemental Movies

Supplemental Movie 1 Time-lapse imaging of UHN6 tumor-organoid Images were taken every 45 minutes for 10 days (See Supplemental Methods for details)